Computational Analysis of Large-Scale Unsteady Flow Past a Circular Cylinder in a Confined Open Vertical Channel

Noor Mohsin Jasim*

Abstract— This paper focuses on the on the analysis of two- dimensional dynamic characteristics of the velocity and pressure fields of transient incompressible laminar wakes behind a circular cylinder in a large scale confined vertical channel with upward flow. Three test cases are selected to be investigated and compared physically and numerically. The laminar flow in a large scale for low Reynolds number Re = 20,40 and 100 are simulated. The flow equations are written in terms of Naiver-Stokes formulation are solved using two-dimensional finite volume method (FVM). The benefit of using unsteady flow condition is to evaluated the vortex behind the circular body (cylinder) in a lrage computational domain. The capabilities of these equations are to compute drag and lift coefficients in real large confined open channel. Due to the shortage in experimental data the obtained results are validated by the reasonable capturing prediction procedure.

Keywords—Laminar flow, Open vertical channel, Flow over cylinder, Large scale.

1 Literature Survey:

Heat transfer and fluid flow over a circular cylinder is a common topic which has been investigated quite thoroughly in the last few decades, primarily due to its applicability to many engineering applications. The confined wall, cylinder shape and nature of flow have the effectiveness on past flow. These configuration and flow properties have a considerable influence on the flow geometric properties and turbulent features.

Flow and heat transfer over a circular cylinder has been known and the subject of research for a long time. Kai Liu et al. [1] performed an experimental study to explore the effect of a splitter on flow structure behind a cylinder placed in a confined channel. The circular cylinder with a diameter D=30 mm was symmetrically placed in the confined channel. The flow visualization was investigated using the PIV measurements technique. In this study, two values of Re was applied, 2400 and 3000 with different values of the control elements of the splitter plate length, ranging between L/D=0 to 1.5. The result showed that the stabilization of wake turbulences was significantly influenced by the splitter plate. It was clearly seen that there was a significant enhancement in the flow structures in the case of the shorter splitter plate length (L/D=0.5 and 0.75) as well as a decrease in the vortex frequency in contrast with bare cylinder cases. For longer splitter length of (L/D) =1, 1.25 & 1.5 cases, the snapshot proper orthogonal decomposition analysis showed the generation of a secondary vortex. Furthermore, at Re=3000, the stabilizing effect of a splitter plate was clearly seen than that at a lower Re. Ricky Tiong et al. [2] used various types of nanofluids such as Al2O3, CuO, SiO2, and TiO2 to investigate the influence of aiding buoyancy on 2-D laminar stream around a circular cylinder. The study was carried out numerically using the finite volume method based on SIMPLEC technique. Different values of the flow parameter of Ri , Re, & blockage ratioB were applied. Different sizes of the nanoparticles is also studied dp. They confirmed that the highest heat transfer coefficient was achieved with Al2O3 nanofluid type compared to another type of nanofluids. The highest Nusselt number (Nu) also occurs at φ=10% (nanopaticle concentration). Besides, the Nusselt number is higher for lower nanoparticles size (dp=25nm) while a higher blockage yields higher Nusselt number.

Later, Dipankar Chatterjee and Mohammad RAJA [3] presented a numerical study of fluid and heat transfer over set of cylinders with a square shape in row in a vertical flow. Their study is conducted for the blockage ratios = d/L = 00.1, 0.25, and 0.5 at Re = 100 and Pr=0.7 for different values of the Richardson number ranges from –1 to +1. The commercial code FLUENTTM was used to run the simulation. In the cases of the opposed buoyancy (Ri < 0), periodic vortex shedding is clearly seen while it is stopped for the aided buoyancy cases. The results also showed that the shedding frequency is higher for higher blockage ratio compared to that for the lower one. In another study, the effect of aiding/opposing buoyancy at different values of the Ri , Re & Pr is also studied by Atul Sharma and V. Eswaran [4] to examine the influence of confined channel on the perpendicular flow and thermal flux properties around a square cylinder. They found that the minimum heating required for the suppression of vortex shedding decreases with increasing blockage ratio while it starts to in-

* *Lecturer Noor Mohsin Jasim, University of Kufa\ Faculty of Engineering \ Mechanical Department\ E-mail: Noorm.alhasnawi@uokufa.edu.iq*

crease with any increase in blockage ratio above 30 %. Their results also presented the effect of buoyancy and channel-confinement on different parameters such as the pumping power, recirculation length, drag and lift coefficient.

Furthermore, S. Moulai1 et al. [5] reported a numerical study of 2D steady flow & heat transfer flow and over a square cylinder under the effect of the buoyancy aided in a confined channel. The finite volume method is used to solve the governing equations. The open source OpenFoam® code is used to run the numerical simulation for various values of the Reynolds number and the Richardson number at a fixed values of blockage ratio and Prandtl number. It is observed from the results that increasing the Grashof number (Gr) causes a decrease in the wake region while its size increases as the Reynolds number increases. It is also noticed that the Nusselt number strongly depends on both (Re) & (Gr). The Nusselt number on the front side increases with an increase in the Reynolds number while the Nusselt number on the side faces increases with increasing the Grashof number.

A study is done by Adnan A. Abdul Rasool et al. [6] to predict and measure the heat transfer by natural convection around a vertical arrangement of a square bars close to a insolated wall. The flow and temperature fields are studied for different values of horizontal distance ratio ranging from 0.125 to 3.0 and different values of vertical distance ranging from 1.5 to 4. The Rayleigh number effect is also examined in this study with various values in the range of ($1.26\times106 < Ra < 6.6\times106$). They found that the Nusselt number strongly depends on the location of the bars in the arrangement, the distances among the bars and the space from side wall. It is noticed that increasing the ratio of H/D value leads to a significant enhancement in the Nusselt number of every rod because of the chimney influence. It is also found when H/D value increases (H/D> 1). Dipankar Chatterjee [7] predicted the heat transfer of a 2D incompressible steady state flow over cylinders arranged in a confined space. The fixed parameter of (d/H) in the difference ranges of Reynolds and Richardson numbers with a fixed Prandtl number are conducted in their study. It is observed that a greater eddies zone appears backwards the cylinders at higher values of (Re) for buoyancy opposed compared to that for buoyancy-aided. A higher value of Re leads to reduce the CD and enhance the Nu.

Amit Dhiman et al. [8] explored the role of aiding buoyancy on behavior of flow and thermal properties around a cylinder at low Reynolds numbers and various values of Re, BR and Ri. The results showed that the total CD increases with both Ra and BR but it decreases with Re. The average Nu increases with both Re and Ra. Gurunath Gandikota et al. [9] studied the effect of buoyancy on the two-dimensional laminar flow over a circular cylinder fixed in a vertical channel for several values of Reynolds and Richardson numbers and two different values of the blockage ratios (B=0.02 and 0.25). It is found that for both cases of the channel confined and unconfined cases, the critical Richardson number increases as Reynolds number increases in the chosen range. It is also seen that reducing the blockage ratio leads to increase the critical Ri at any value of Re. In addition, higher values of blockage ratio enhance the Nusselt number.

Moulai S. et al. [10] also examined the effect of aiding buoyancy by mixed convection from a horizontal cylinder in the vertical channel at Re, Richardson number & Grashof number for a fixed values of Prandtl and blockage ratio. The finite volume method is used to solve the governing equations using the commercial code Open FOAM. It is observed from the results that increasing the (Gr) causes a reduction in the size of wake region while its size increases as the Reynolds number increases. It is also noticed that the Nusselt number strongly depends on both (Re) and (Gr). The Nusselt number on the front face of the obstacle increases with an increase in the Reynolds number while the Nusselt number on the side faces increases with increasing the Grashof number. Neha Sharma et al. [11] performed a numerical simulation to study the behavior of non-Newtonian power-law flow and heat transfer past a cylinder under the effect of buoyancy in a vertical channel for various values of the Reynolds number, Re=1–40; Richardson number, Ri=0–1, and blockage ratio, BR=25%–50% at a fixed value of Prandtl number of 50. It is concluded that the aiding buoyancy significantly enhances the heat transfer rate as well as increasing the drag coefficient. On the other hand, increasing the shearing-thinning tendency leads to increase the Nusselt number and reduce the drag coefficient.

A. K. Saha[12] examined a laminar and incompressible flow and heat transfer characteristics of unsteady natural convection over a square cylinder placed symmetrically in a vertical parallel plate channel. In this study, a wide range of (Grs) is conducted with a fixed value of Prandtl number. The results showed that when Grs exceeds the value of 3.0 104, the natural convection flow behavior becomes unstable. It is observed that the drag force on the cylinder decreases with the increase in Grashof number. Furthermore, heat transfer from a square cylinder is found to be higher than that from a circular cylinder and the heat transfer is significantly enhanced when the flow turns to unsteady state. Besides the highly valuable studies outlined above, exhaustive numerical study was performed by Katsuhisa Noto and Kyohsuke Fujimoto [13] using

IJSER

the DNS technique to simulate and analyze the flow and heat transfer of a vertical mainstream of air over a heated circular cylinder wake. The air flow stream is at Reynolds number of 300 and Richardson number of 0.3. The results revealed that the buoyancy has a positive effect on the flow and heat transfer behavior. The buoyancy produces a higher upward velocity u in the whole wake. The three-dimensionality becomes more dominant in the nearwake due to the buoyancy effect. The buoyancy also suppresses the Karman vortex street in the farwake. Another effect of the buoyancy in the farwake is observed by suppression of the 3-D and vortex dislocation.

Suresh Singh et al. [14] carried out an unsteady mixed convection flow past a heated/ cooled circular cylinder positioned inside an insulated vertical channel. A novel finite volume technique is used to solve the governing equation of the current fluid flow regime and heat transfer field. They confirmed that no vortex shedding can be seen at a critical Ri=0.15. A strong vortex is observed when the value of Richardson number is lower than 0.15. At this value of Ri, the vortex shedding is quite prominent. On the other hand, For Ri > 0.15, the vortex shedding does not appear in the flow regime. A significant enhancement in the heat transfer rate can also be found with any increase in the value of Ri number above 0.15.

2 GOVERNING EQUATIONS:

The equations for fluid flow are the Navier-Stokes equations. The flow is assumed to be a steady, laminar and incompressible flow. When the density of a viscous fluid is constant, the equations are sufficient to model the flow in general form can be described in terms of the conservation of mass equation, or commonly known as the continuity equation. The continuity equation in divergence form, can be written as:

Continuity equation:

$$\frac{\partial U}{\partial X}+\frac{\partial U}{\partial Y}=0 \tag{1}$$

X-momentum equation:

$$\frac{\partial U}{\partial \tau}+\frac{\partial (UU)}{\partial X}+\frac{\partial (UV)}{\partial Y}=\frac{\partial P}{\partial X}+\frac{1}{\mathrm{Re}}\left(\frac{\partial^2 U}{\partial X^2}+\frac{\partial^2 U}{\partial Y^2}\right) \tag{2}$$

Y-momentum equation:

$$\frac{\partial U}{\partial \tau}+\frac{\partial (UU)}{\partial X}+\frac{\partial (UV)}{\partial Y}=\frac{\partial P}{\partial Y}+\frac{1}{\mathrm{Re}}\left(\frac{\partial^2 U}{\partial X^2}+\frac{\partial^2 U}{\partial Y^2}\right) \tag{3}$$

where ρ , $\vec{V}$,∇ are the density, velocity vector and gradient operator. The conservation of momentum equation is derived using the Newtons second law applied to a fluid passing through an infinitesimal control volume. It is written in divergence form as:

$$\nabla.(\rho\vec{V}\vec{V})=\nabla.(\mu\nabla\vec{V})+\vec{S}+\nabla P \tag{4}$$

where μ, $\vec{S}$ and P are the fluid viscosity, the source term due to any external forces and the pressure gradient.

3. PROBLEM DESCRIPTION AND BOUNDARY CONDITIONS

The configuration for the open confined channel of the physical problem used in this study along with the considered coordinates system used is shown in (Fig. 1). The flow is approximated by considering the laminar and incompressible flow and fully developed velocity profile at the inlet. The system of interest is selected air as the fluid across an infinitely long circular cylinder of diameter (D=1m) inside a confined channel. The open confined channel flow cases are obtained when no-slip wall boundary conditions are applied to the two adiabatic channel walls of finite length of (h=22 meters) are placed vertically and two placed horizontally at a distance of (x=2 meters) from each side of the center of the cylinder. As mentioned above, the assumption of the fluid enters the channel under fully developed conditions. The three test cases are set up using constant fluid properties and the boundary conditions. Three runs are made using different values of viscosity which permit to use three various of (Re) (Re =20, 40, & 100) with constant inlet vertical velocity of 1 m/sec at the inlet. At the outlet, the boundary condition is used with the flow exit, is treated as a zero-normal-gradient outlet boundary.

4 RESULTS AND DISCUSSIONS

The drag force is referring here to the forces which act on any body object in the direction of the relative velocity for the fluid flow. In addition, the total drag coefficient is calculated here by summing of friction drag and pressure drag coefficients. Figure3 shows the temporal variation of the total drag coefficient along the channel. As expected, the total drag coefficient is found to increase with the increasing Reynolds number. The total lift coefficient presented in Figure 4. It obviously follows the same trend as the total drag coefficient, for the given Reynolds numbers. As Reynolds number increases, the total lift coefficient decreases due to a decrease in the pressure difference above and below the circular cylinder. Consequently, Figure 5 shows the pressure coefficient along the centerline of the vertical channel. The pressure difference between cylinder surfaces (top & bottom) decreases as Reynolds number increasing, leading to decrease of the cylinder lift. Pressure difference between top and bottom cylinder degrading until it

IJSER

reached the open end.

Figure 6 shows the X-velocity gradient at the centerline of the channel. It express that the X-velocity components increases as Reynolds number increase, because of there is a reducing in the pressure over the surface of the cylinder which works as an obstacle. Figure 7 shows the contour plots for the X-velocity for different Reynolds numbers. These plots offer the terminated effect for the velocity near the surface of the cylinder as Reynolds number increased. On the contrary, the Y-velocity gradient exhibits the opposite trend. Figure 8 shows the Y-velocity gradient at the centerline of the channel. Furthermore, as the fluid velocity in the space between the cylinder and the channel wall decreased with Reynolds number increasing as well as the velocity in the wake region decreased. Figure 9 shows the contour plots for the Y-velocity for different Reynolds numbers. These plots explain that the maximum Y-velocity can be found between the space between the cylinder and the channel wall. Figure 10 demonstrates instantaneous contours of stream function at different Reynolds number. Typically those streamlines show complete understanding of vortex shedding with the increasing in the value of Reynolds numbers. At Re =20 and 40, it can be seen that there is no big differences in the streamlines to offer the periodic shedding, whereas at Re = 100 a complete asymmetric unsteady recirculation can be observed. Figure 11 shows the vorticity magnitude at different low Reynolds number. At low Reynolds number(Re=100), the vorticity magnitude is pushed into the wake region and extended vertically away from the boundary layers of the cylinder. It can be noticed that the diffusion of vorticity magnitude away from the shear layers due to the viscous action.

5 CONCLUSIONS

The large scale problem of the unsteady laminar open confined vertical channel flow past a circular cylinder at low Reynolds numbers of 20, 40 & 100 is numerically simulated using 2-D finite volume method. The most important conclusions extracted from results are:

1. The total drag coefficient is found to increase with the increasing Reynolds number.
2. As Reynolds number increases, the total lift coefficient decreases due to a decrease in the pressure difference above and below the circular cylinder.
3. The vortex shedding with the increasing in the value of Reynolds numbers. At Re =20 and 40, it can be seen that there is no big differences in the streamlines to offer the periodic shedding, whereas at Re = 100 a complete asymmetric unsteady recirculation can be observed.
4. At low Reynolds number, the vorticity magnitude is pushed into the wake region and extended vertically away from the boundary layers on the cylinder.

6 REFERENCES

[1] Kai Liu, Jianqiang Deng and Mei Mei. (Experimental study on the confined flow over a circular cylinder with a splitter plate). Flow Measurement and Instrumentation 51(2016) 95–104.

[2] Ricky Tiong Hieng Bing and Hussein A. Mohammed.(Upward Laminar Flow Around A Circular Cylinder Using Nanofluids). Journal of Purity, Utility Reaction and Environment Vol.1 No.9,November (2012), 435-450.

[3] Dipankar Chatterjee , and Mohammad RAJA . (MIXED CONVECTION HEAT TRANSFER PAST IN-LINE SQUARE CYLINDERS IN A VERTICAL DUCT). THERMAL SCIENCE: Year 2013, Vol. 17, No. 2, pp. 567-580.

[4] Atul Sharma , and V. Eswaran . (Effect of channel-confinement and aiding/opposing buoyancy on the two-dimensional laminar flow and heat transfer across a square cylinder). International Journal of Heat and Mass Transfer Volume 48, Issues 25–26, December 2005, Pages 5310-5322.

[5] S. Moulai1, A. Korichi1 and G. Polidori. (Aided Mixed Convection past a Heated Square Cylinder at Low Blockage Ratio). Journal of Applied Fluid Mechanics, Vol. 9, No. 1, pp. 303-310, (2016).

[6] Adnan A. Abdul Rasool, Mohanad Al Thaher, Jalal M. Jalil, and May Al Fahdawi. (Effect of a Side Wall on the Natural Convection Heat Transfer from a Vertical Row of Horizontal Square Rods). Arabian Journal for Science and Engineering, February 2014, Volume 39, Issue 2, pp 1313–1323.

[7] Dipankar Chatterjee. (MIXED CONVECTION HEAT TRANSFER FROM TANDEM SQUARE CYLINDERS IN A VERTICAL CHANNEL AT LOW REYNOLDS NUMBERS). Journal Numerical Heat Transfer, Part A: Applications An International Journal of Computation and Methodology ,Volume 58, Pages 740-755, (2010).

[8] Amit Dhiman, Neha Sharma and Surendra Kumar . (Buoyancy-aided momentum and heat transfer in a vertical channel with a built-in square cylinder). International Journal of Sustainable Energy, Vol. 33, No. 5, pp 963–984, (2014).

[9] Gurunath Gandikota, Sakir Amiroudine, Dipankar Chatterjee, and Gautam Biswas . (THE EFFECT OF AIDING/OPPOSING BUOYANCY ON TWO-DIMENSIONAL LAMINAR FLOW ACROSS A CIRCULAR CYLINDER). Numerical Heat Transfer, Part A: Applications An International Journal of Computation and Methodology , Volume 58: pages 385–402, (2010).

[10] Moulai S, Korichi A. , Fohanno S. and Polidori G. (BUOYANCY-ASSISTED MIXED CONVECTION FLOW OVER A HEATED SQUARE CYLINDER IN A VERTICAL CHANNEL). 10th International Conference on Heat Transfer, Fluid Mechanics and Thermodynamics, 14 – 26 July 2014 , Orlando, Florida.

[11] Neha Sharma, Amit Dhiman, and Surendra Kumar. (NON-NEWTONIAN POWER-LAW FLUID FLOW AROUND A HEATED SQUARE BLUFF BODY IN A VERTICAL CHANNEL UNDER AIDING BUOYANCY). Numerical Heat Transfer, Part A: Applications An International Journal of Computation and Methodology , Volume 64: Pages 777–799, (2013).

[12] A. K. Saha. (UNSTEADY FREE CONVECTION IN A VERTICAL CHANNEL WITH A BUILT-IN HEATED SQUARE CYLINDER) . Numerical Heat Transfer, Part A: Applications An International Journal of Computation and Methodology , Volume 38: Pages 795–818, (2000).

[13] Katsuhisa Noto, and Kyohsuke Fujimoto . (NUMERICAL COMPUTATION FOR BUOYANCY EFFECT ON THREE-DIMENSIONALITY AND VORTEX DISLOCATION IN

HEATED WAKE WITH VERTICAL MAINSTREAM). Numerical Heat Transfer, Part A: Applications An International Journal of Computation and Methodology , Volume 51: Pages 541–572, (2007).

[14] Suresh Singh, G. Biswas, and A. Mukhopadhyay. (EFFECT OF THERMAL BUOYANCY ON THE FLOW THROUGH A VERTICAL CHANNEL WITH A BUILT-IN CIRCULAR CYLINDER). Numerical Heat Transfer, Part A: Applications An International Journal of Computation and Methodology , Volume 34: Pages 769–789, (1998).

[15] S. Lee, D. Tanaka, J. Kusaka, and Y. Daisho. Effects of diesel fuel characteristics on spray and combustion in a diesel engine; JSAE200224660, Japanese Society of Automotive Engineers: Tokyo, Japan, 2002.

[16] C. S. Lee, S. W.Park, and S. I. Kwon. An Experimental Study on the Atomization and Combustion Characteristics of Biodiesel-Blended Fuels. Energy Fuels,19 (2005), 2201.

[17] Y. Wengiao. Computational modelling of nitrogen oxide Emissions from biodiesel based on accurate fuel properties. W. Yuan, PhD Dissertation, University of Illinois at UrbanaChampaign. Department of Agricultural and Biological Engineering, 2006.

[18] C. A. W. Allen. Prediction of biodiesel fuel atomization characteristics based on measured properties. PhD Dissertation, Dalhousie University-DALTECH, Halifax, Canada, 1998.

[19] K. Yamane, A. Ueta, and Y. Shimamoto. Influence of Physical and Chemical Properties of Biodiesel Fuel on Injection, Combustion and Exhaust Emission Characteristics in a DI-CI Engine, The Fifth International Symposium on Diagnostics and Modeling of Combustion in IC Engines COMODIA, Nagoya, Japan, July 14, 2001.

[20] Su Han Park, Hyung Jun Kim, Hyun Kyu Suh and Chang Sik Lee. A study on the fuel injection and atomization characteristics of soybean oil methyl ester (SME). International Journal of Heat and Fluid Flow, 30 (2009), 108–116.

[21] Su Han Park, Hyung Jun Kim, Hyun Kyu Suh and Chang Sik Lee. Experimental and numerical analysis of spray-atomization characteristics of biodiesel fuel in various fuel and ambient temperatures conditions. International Journal of Heat and Fluid Flow, 30 (2009), 960970.

[22] Xiangang Wang , Zuohua Huang , Olawole Abiola Kuti , Wu Zhang and Keiya Nishida. Experimental and analytical study on biodiesel and diesel spray characteristics under ultra-high injection pressure. International Journal of Heat and Fluid Flow, 31 (2010), 659666.

[23] S. Som , D.E. Longman , A.I. Ramrez and S.K. Aggarwal. A comparison of injector flow and spray characteristics of biodiesel with petrodiesel. Fuel, 89 (2010), 40144024.

[24] J. C. Beck and A. P. Watkins. On the development of a spray model based on drop-size moments. Proc. R. Soc. Lond., A(459)(2003),1365-1394.

[25] F. H. Harlow and A. A. Amsden. Numerical calculation of multiphase fluid flow. Journal of Computational Physics. 17(1975), 19–52.

[26] J. C. Beck and A. P. Watkins. On the development of a spray model based on drop-size moments. Proc. R. Soc. Lond., A(459):13651394, 2003a.

[27] W.K Melville and K.N.C. Bray. A model of the two-phase turbulent jet International Journal of Heat and Mass Transfer v.22(1979), 647–656 .

[28] J. C. Beck and A .P. Watkins. The droplet number moments approach to spray modelling: The development of heat and mass transfer sub-models. Int. J. of Heat and Fluid Flow, 24(2003),242-259.

[29] A.A. Amsden, P.J.ORourke and T.D. Butler. KIVA-II: A computer program for chemically reactive flows with sprays, Technical Report LA-11560-MS, Los Alamos National Laboratory, 1989.

[30] B. E. Launder and D. B. Spalding. Mathematical models of turbulence, London academic press, 1972.

[31] A. A. Mostafa and H. C. Mongia. On the modelling of turbulent evaporating sprays:Eulerian versus lagrangian approach. Int. J. Heat and Mass Transfer, 30 (1987).

[32] R.H. Windschitl, http://www.rskey.org/gamma.htm.

[33] H. Hiroyasu and T. Kadota. Fuel droplet size distribution in diesel combustion chamber. SAE, paper 740715.1974.

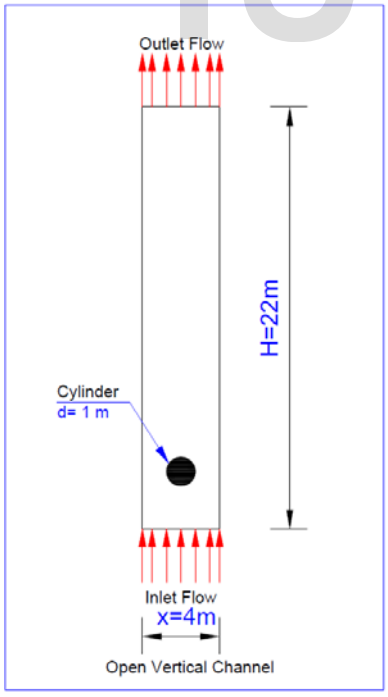

Figure (1): Schematic diagram of the flow field around circular cylinder in a open confined vertical channel.

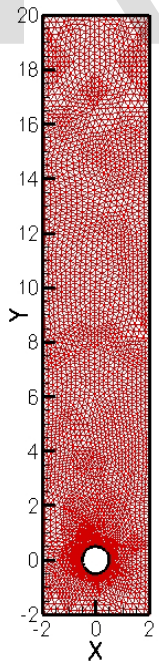

Figure (2): Computational domain.

IJSER

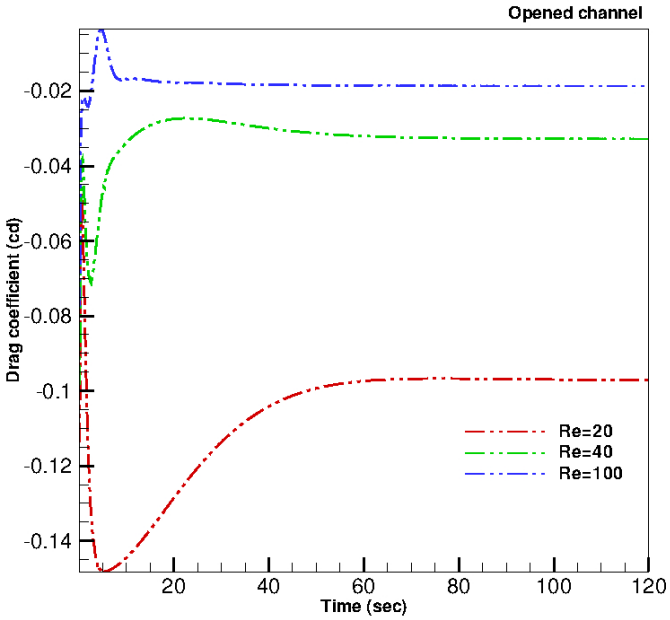

Figure (3): Temporal evolution of drag coefficient for laminar flow past a circular cylinder at different Reynolds number.

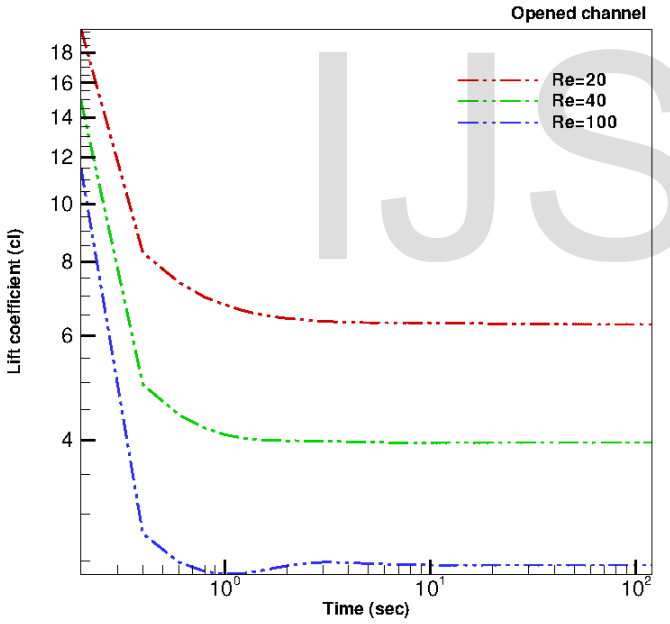

Figure (4): Temporal evolution of lift coefficient for laminar flow past a circular cylinder at different Reynolds number.

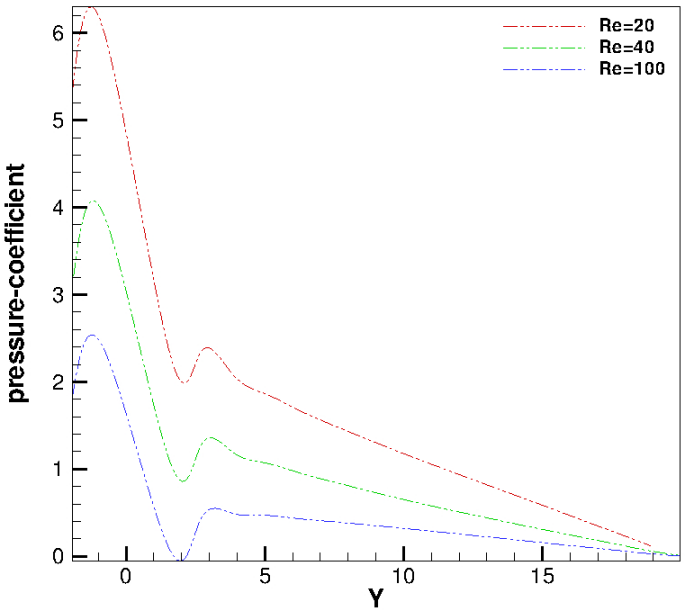

Figure (5): Temporal evolution of pressure coefficient for laminar flow past a circular cylinder at different Reynolds number.

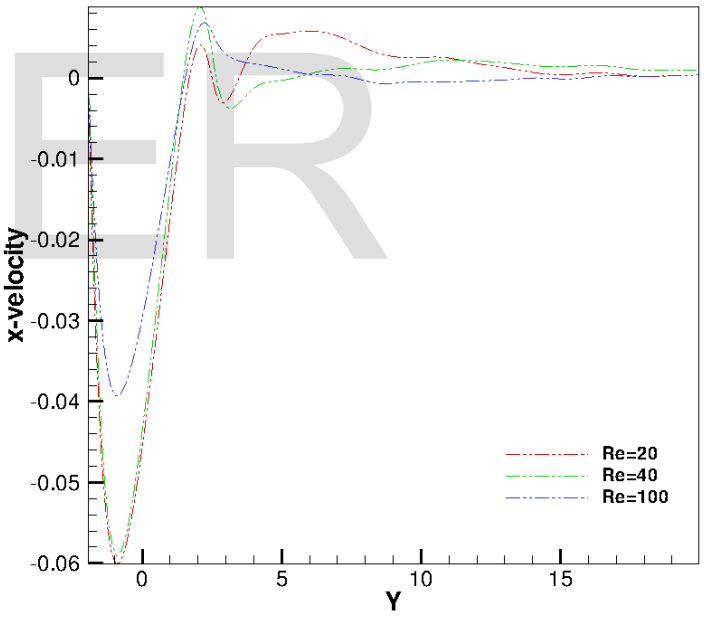

Figure (6): Variation of x-velocity component along Y-distance with different Reynolds number.

IJSER

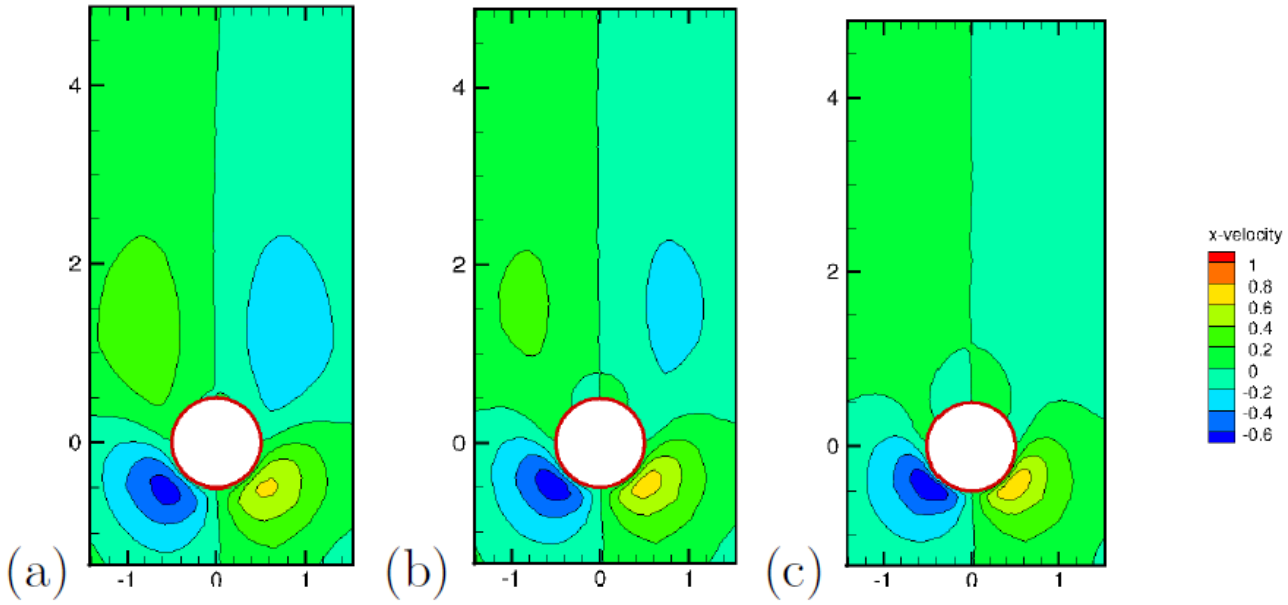

Figure (7): Instantaneous x-velocity component contours for different Reynolds number.

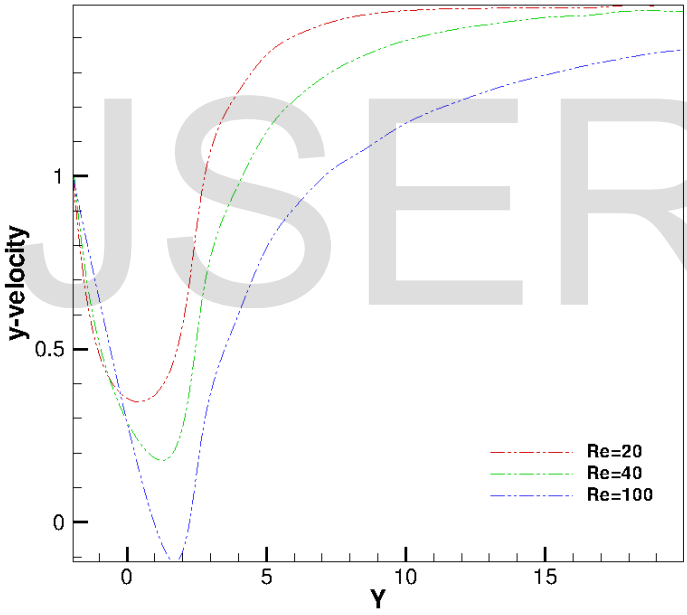

Figure (8): Variation of y-velocity component along Y-distance with different Reynolds number.

IJSER

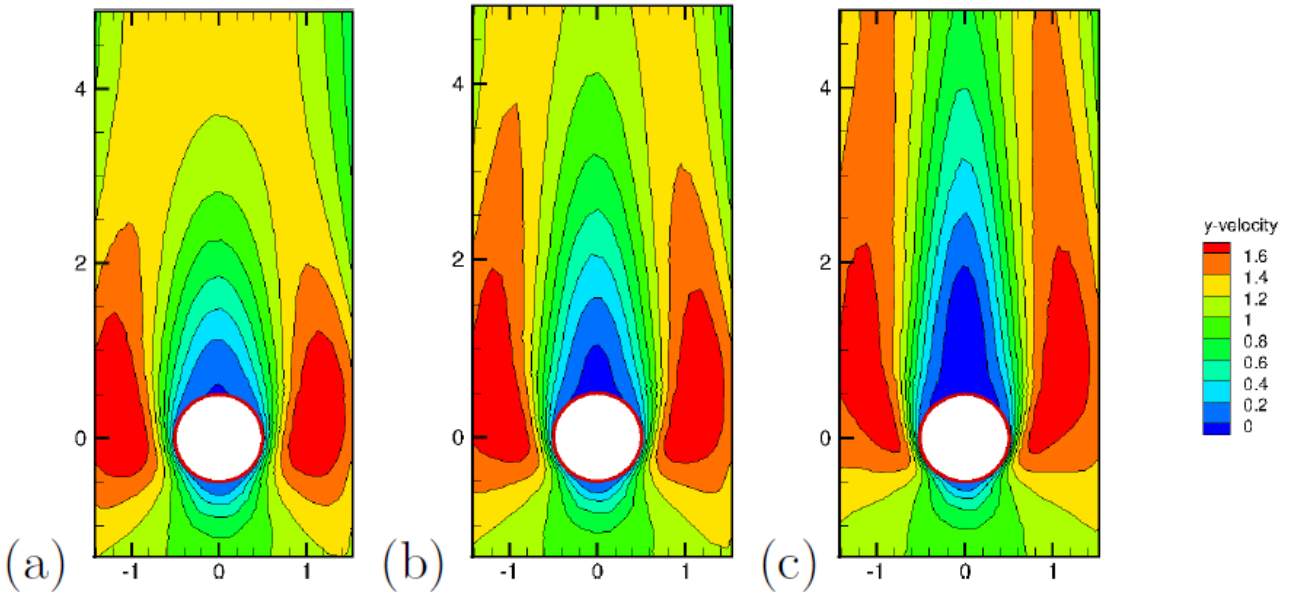

Figure (9): Instantaneous y-velocity component contours for different Reynolds number.

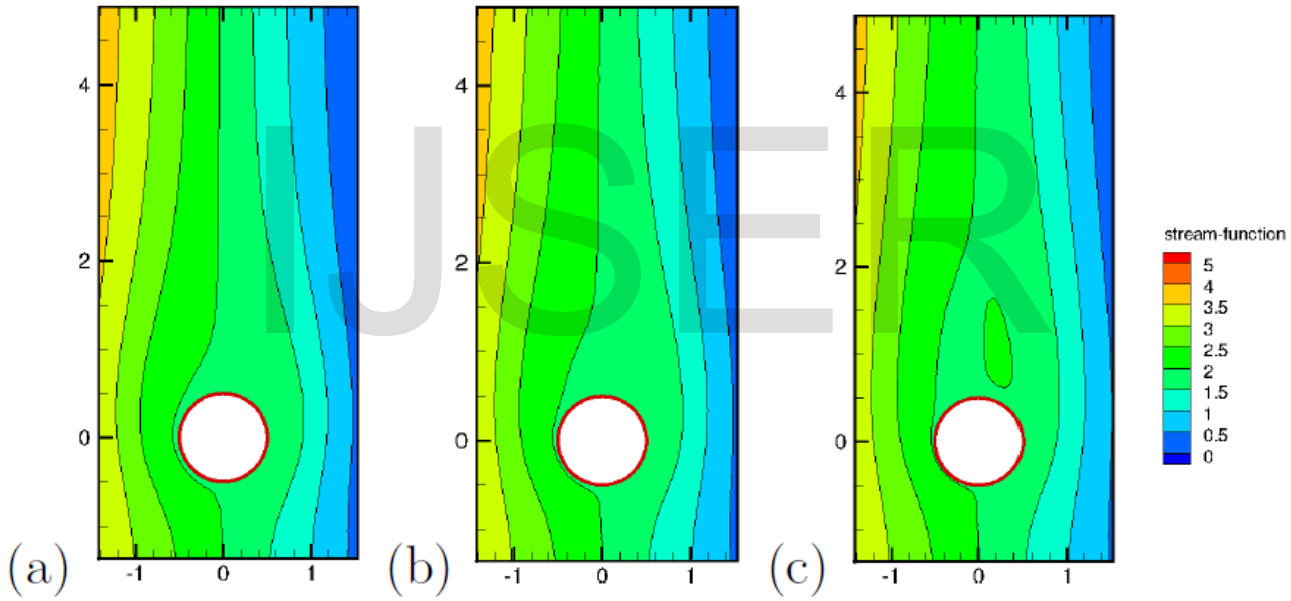

Figure (10): Instantaneous stream- function contours for different Reynolds number.

IJSER

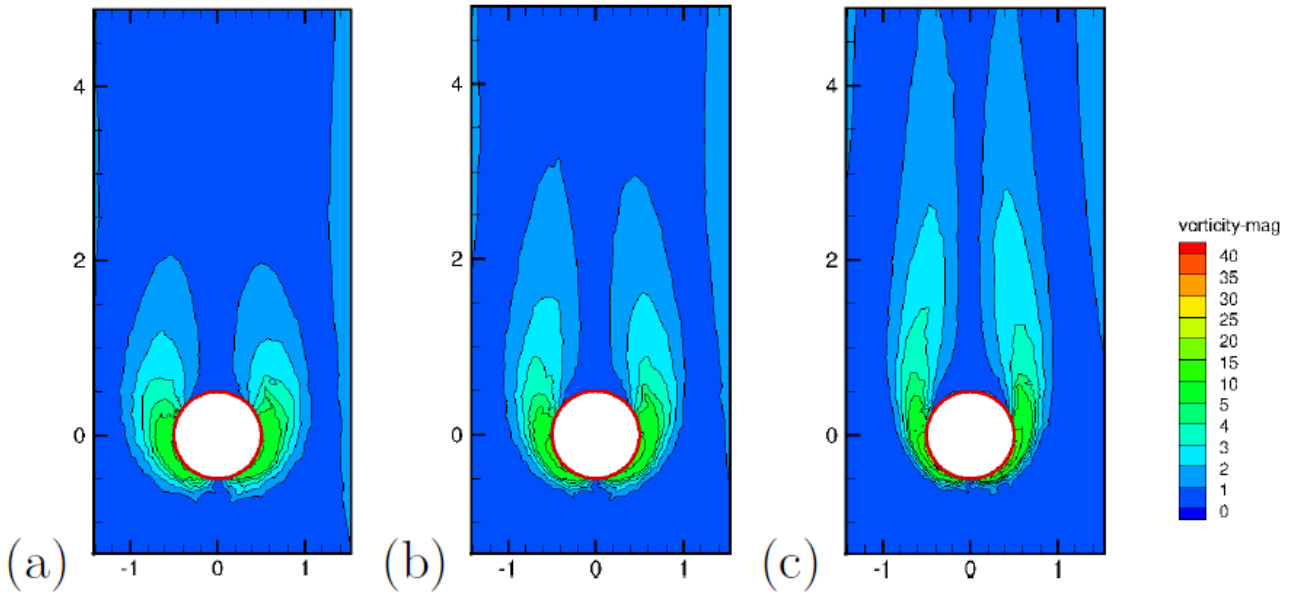

Figure (11): Instantaneous vorticity magnitude contours for different Reynolds number.

IJSER